

Fig. 1: Time average of the global mean surface temperature  $T_s$  (solid line) and of the temperature of the warm ( $\Theta^+$ ) and cold ( $\Theta^-$ ) reservoirs (dashed and dotted lines, respectively).

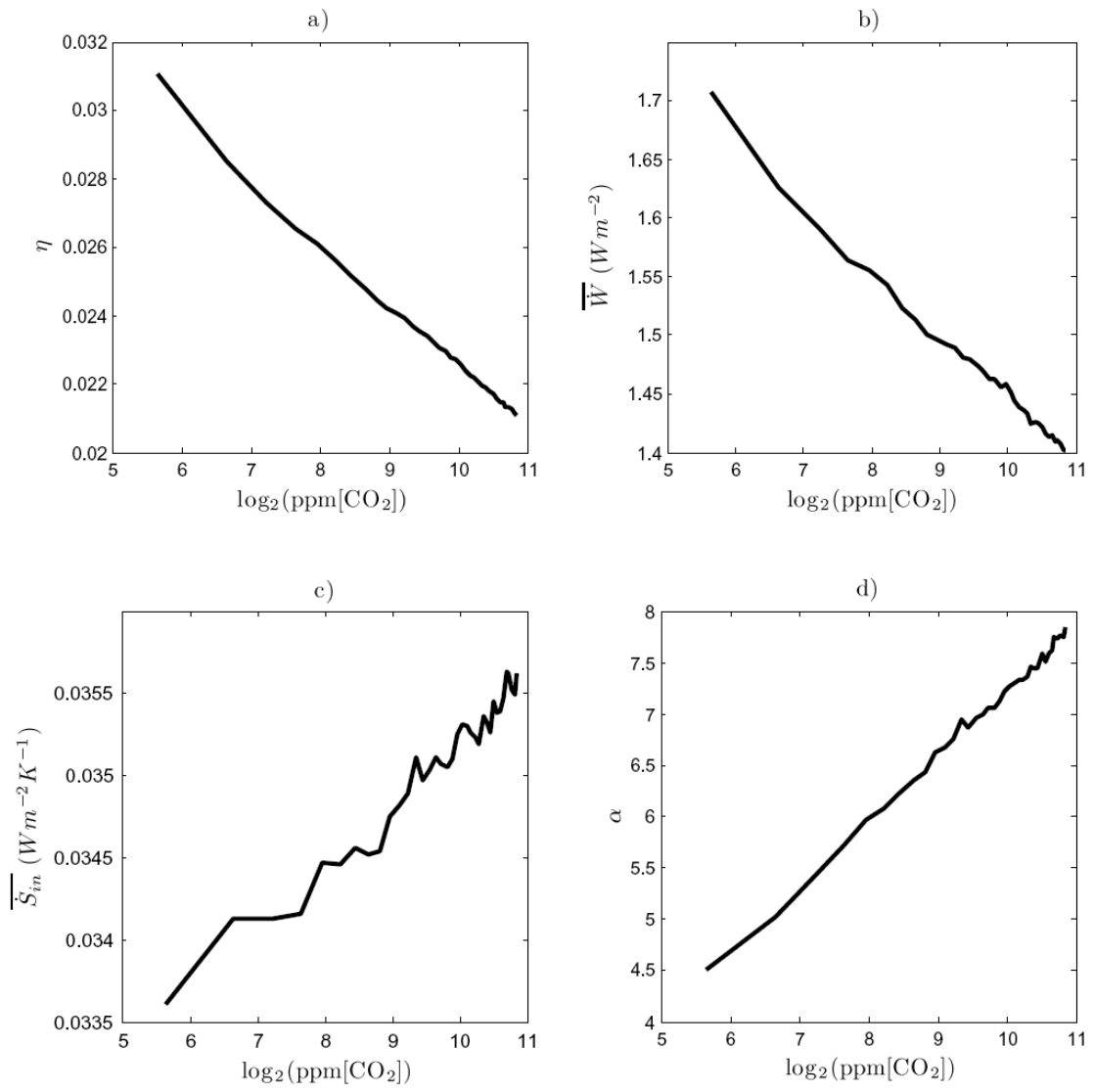


Fig. 2: Generalised climate sensitivities: CO<sub>2</sub> concentration dependence of macroscopic thermodynamic variables. See text for details.

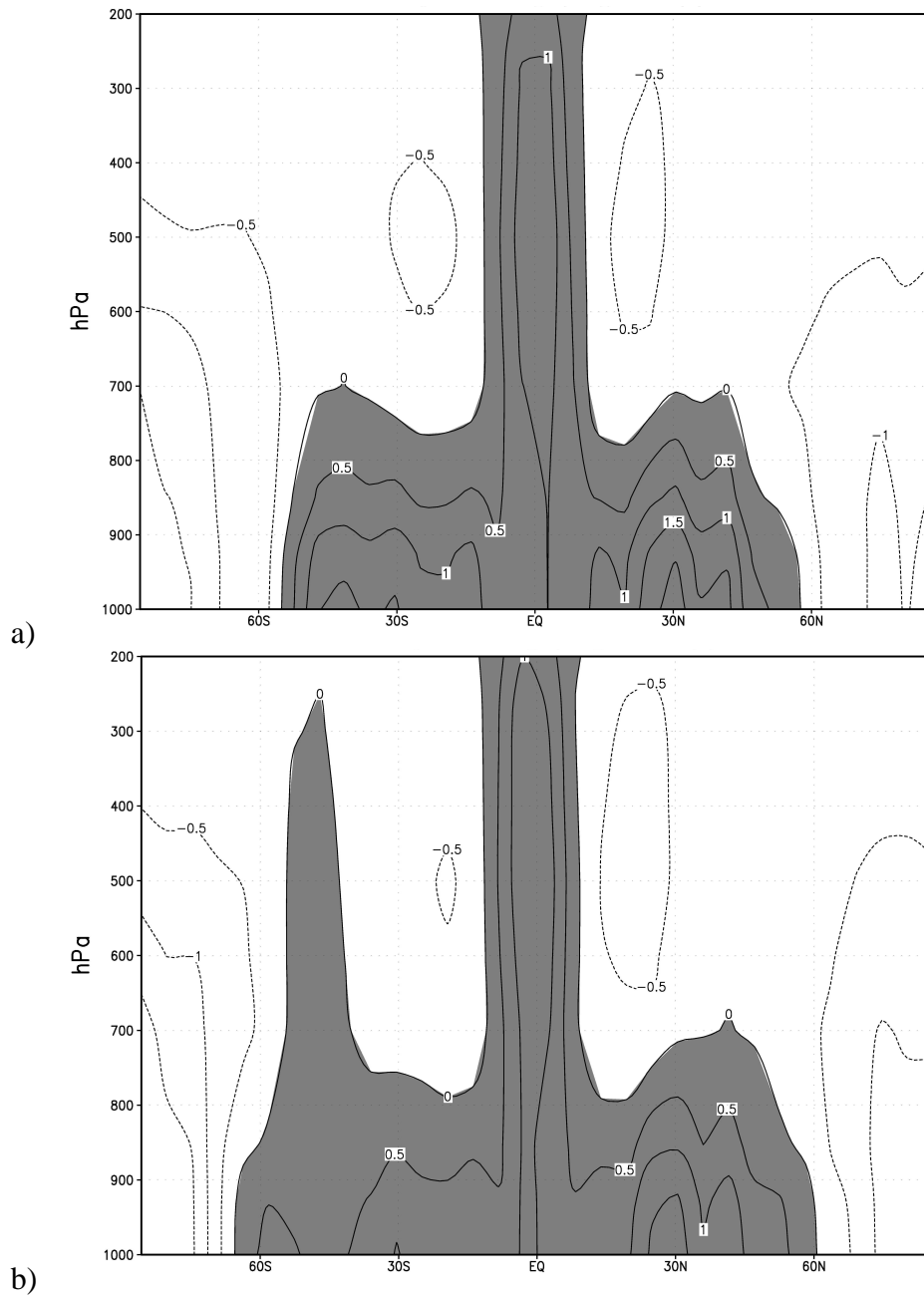


Fig. 3: Zonally and vertically averaged mean heating rates (in K/day) for the 100 (a-c) and 1000 (b-d) ppm CO<sub>2</sub> concentration runs.

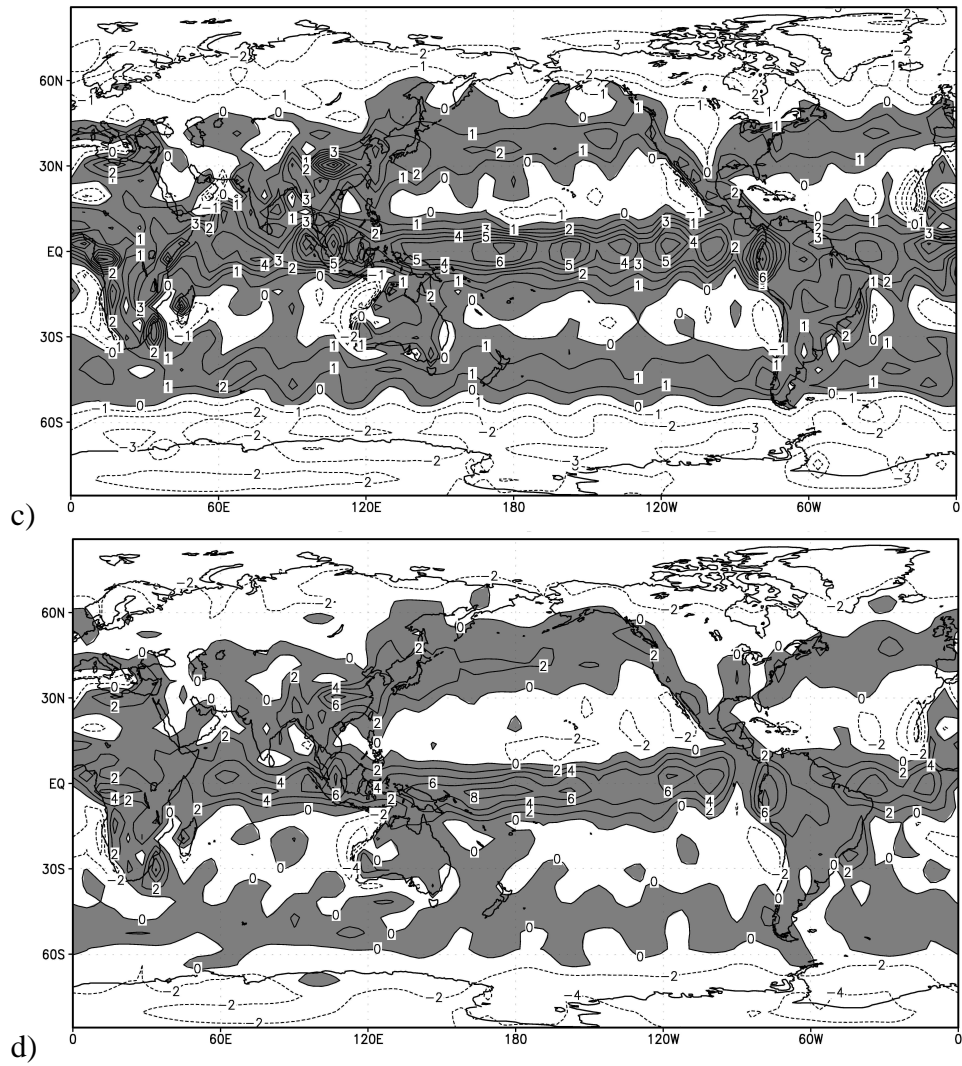


Fig. 4: Vertically averaged mean heating rates (in K/day) for the 100 (a-c) and 1000 (b-d) ppm CO<sub>2</sub> concentration runs.



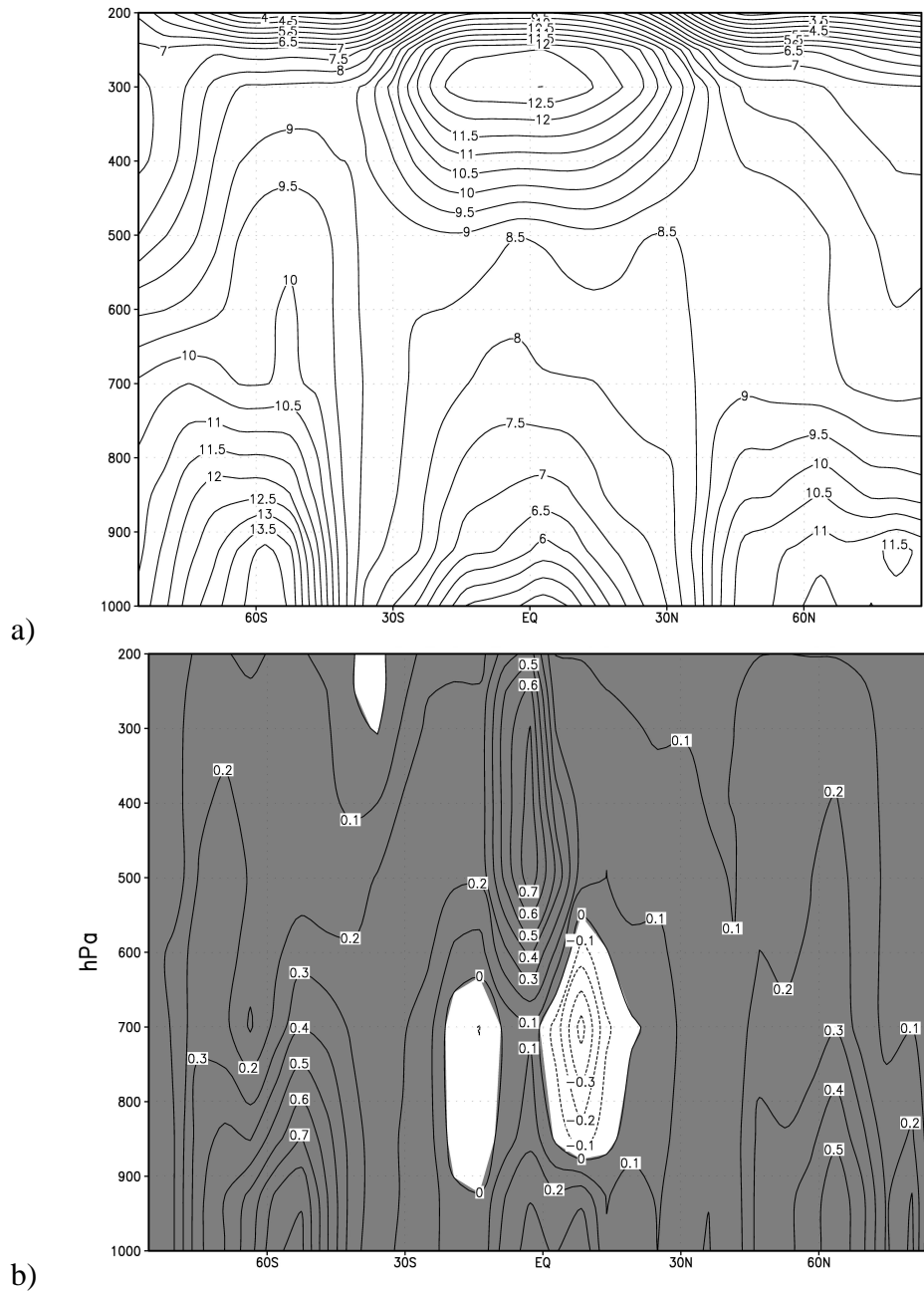
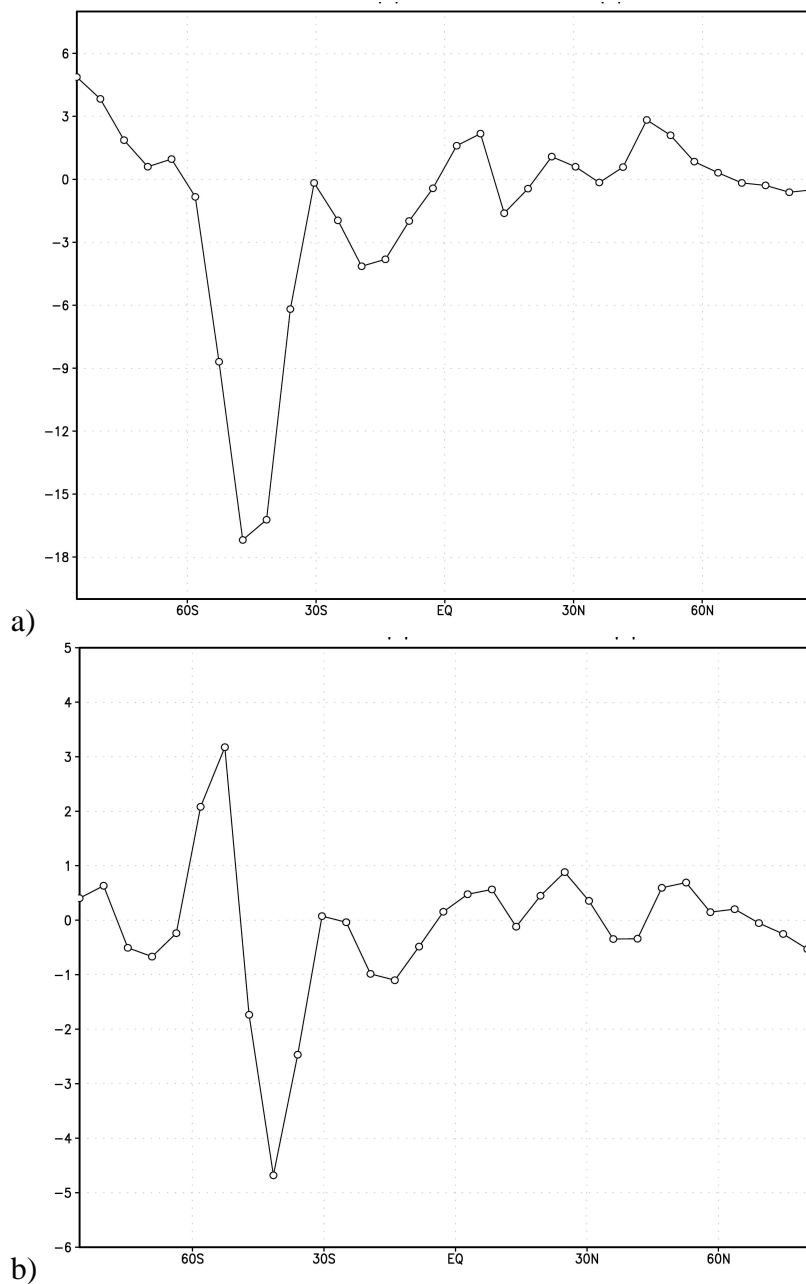


Fig. 5: a) Zonally averaged mean temperature difference between the 1000 ppm CO<sub>2</sub> and 100 ppm CO<sub>2</sub> concentration runs. b) Zonally averaged difference between the 1000 ppm CO<sub>2</sub> and 100 ppm CO<sub>2</sub> concentration runs for the mean heating rates due to the convergence of lateant heat fluxes (in K/day).



a) Zonally averaged difference between the 1000 ppm CO<sub>2</sub> and 100 ppm CO<sub>2</sub> runs for the mean squared velocity (in  $m^2s^{-2}$ ) at the sigma level closest to surface. b) Same as a), but the difference between the 1000 ppm CO<sub>2</sub> and 350 ppm CO<sub>2</sub> runs is shown.